

Nonlinear instability dynamics in a high-density, high-beta plasma

C. S. Corr and R. W. Boswell

Citation: *Physics of Plasmas* **16**, 022308 (2009); doi: 10.1063/1.3074790

View online: <http://dx.doi.org/10.1063/1.3074790>

View Table of Contents: <http://scitation.aip.org/content/aip/journal/pop/16/2?ver=pdfcov>

Published by the [AIP Publishing](#)

Articles you may be interested in

[Instabilities in a capacitively coupled oxygen plasma](#)

Phys. Plasmas **22**, 043515 (2015); 10.1063/1.4918943

[Nonlinear effects of inertial Alfvén wave in low beta plasmas](#)

Phys. Plasmas **22**, 022310 (2015); 10.1063/1.4913229

[Nonlinear dynamic of low-frequency Buneman instability of a current-driven plasma](#)

Phys. Plasmas **12**, 062110 (2005); 10.1063/1.1929367

[Nonlinear Dynamical Analysis of Two Current-Driven Low-Frequency Instabilities in a Magnetised Plasma Column](#)

AIP Conf. Proc. **669**, 719 (2003); 10.1063/1.1594031

[Electron magnetohydrodynamic turbulence in a high-beta plasma. II. Single point fluctuation measurements](#)

Phys. Plasmas **7**, 4457 (2000); 10.1063/1.1314344



PFEIFFER VACUUM

VACUUM SOLUTIONS FROM A SINGLE SOURCE

Pfeiffer Vacuum stands for innovative and custom vacuum solutions worldwide, technological perfection, competent advice and reliable service.

125 YEARS NOTHING IS BETTER

Nonlinear instability dynamics in a high-density, high-beta plasma

C. S. Corr^{a)} and R. W. Boswell

*Space Plasma, Power and Propulsion Group, Research School of Physical Sciences and Engineering,
The Australian National University, Canberra 0200, Australia*

(Received 10 September 2008; accepted 6 January 2009; published online 18 February 2009)

Entrainment and periodic pulling of an ion acoustic instability have been observed in the power spectra of a low-pressure high-beta plasma. The observed nonlinear phenomena can be modeled by using the van der Pol equation with a forcing term. Experimental results of the nonlinear processes are presented. Ion density fluctuations are detected on a negatively biased Langmuir probe for magnetic fields and input powers above 30 G and 900 W at 7.2 MHz respectively, and gas pressure below 1.5 mTorr. This low-frequency instability is observed in the central plasma blue core (argon II emission) and can be controlled by amplitude modulation of the radio frequency input power at frequencies close to the instability frequency. © 2009 American Institute of Physics.

[DOI: 10.1063/1.3074790]

I. INTRODUCTION

Dynamic control of nonlinear systems is a challenging subject in various interdisciplinary fields. Simple mathematical models such as the van der Pol oscillator¹ are often employed to understand the nonlinear dynamical phenomena of physical systems. The van der Pol equation² describes the behavior of an oscillator with a nonlinear damping term.

$$\frac{d^2x}{dt^2} + C(x^2 - 1)\frac{dx}{dt} + x = 0. \quad (1)$$

If the parameter $C=0$ the equation reverts to that describing simple harmonic motion but as the value of C is increased, the system will first enter a limit cycle and will then be heavily damped. For certain values of C van der Pol noted that an irregular noise could be generated. This was one of the first reported discoveries of deterministic chaos.

van der Pol continued his research by adding a harmonic forcing term to describe the oscillations in a triode circuit but found that the model system could also be applied to a broad range of circumstances (the heartbeat considered as a relaxation oscillation, and an electrical model of the heart).³ A number of plasma systems have reported this chaotic type of behavior too and an earlier example in WOMBAT (waves on magnetized beams and turbulence) has been published.⁴ Briefly, the unstable system has an exponential growth and a quadratic damping which, when sufficiently large, will flip the growing instability back to a small amplitude so that it restarts its cycle. This particular instance showed the well known bifurcation path to chaos. The forced van der Pol equation describes a very similar system as shown in another experiment in WOMBAT which displayed subharmonic generation.⁵

Low-frequency fluctuations in magnetized plasmas are easily observed, however, it is not so easy to clarify their origin. Typically, these low-frequency phenomena are identified as drift waves, ion acoustic waves⁶ or as Kelvin–Helmholtz instabilities.⁷ The drift wave instability plays an

important role in turbulent transport of the magnetized fusion plasmas due to the presence of density and temperature gradients.^{8–10} A fluid with a gradient in mass flow velocity can be subject to the Kelvin–Helmholtz instability. These two types of instability can be easily confused since they are both of low frequency and they both arise spontaneously when the magnetic field is sufficiently high. However the two oscillations can be distinguished by their localization in space. The amplitude of drift waves is peaked in the region of large density gradient, while the Kelvin–Helmholtz instability is peaked in the velocity shear region. Additionally, the instability may be the driving force for a resonant wave in the plasma discharge cavity, and for the present high-beta experiment that could be an Alfvén wave or an ion acoustic wave, or a combination of both, the magnetosonic/fast Alfvén wave.

The successful control of unstable behavior in plasmas has attracted great interest over the years. Mechanisms for suppressing various kinds of internal instabilities in magnetized and unmagnetized plasma systems have been investigated.^{11–16} Keen and Fletcher^{12,13} investigated the suppression of an ion acoustic instability by inducing density perturbations at various frequencies close to and far away from the instability frequency. They termed it synchronous and asynchronous suppression, respectively. Boswell and Christiansen¹¹ employed a remote optical feedback technique to stabilize an ion-acoustic-type instability while Klinger *et al.*¹⁴ investigated the van der Pol behavior of a periodically driven, self-oscillating thermionic discharge. More recently, Block *et al.*¹⁶ investigated the synchronization of drift waves in a low density (10^{10} cm⁻³) linear plasma device.

Helicon wave discharges have attracted great interest in the past decades due to their ability to produce high plasma densities.¹⁷ Although there have been many publications on helicon discharges, there have been few on low-frequency oscillations and in particular the control of these instabilities. Light *et al.*^{18,19} observed a low-frequency electrostatic instability only above a critical magnetic field and identified it as a mixture of drift waves and Kelvin–Helmholtz instability. Degeling *et al.*²⁰ observed relaxation oscillations in the kilo-

^{a)}Electronic mail: cormac.corr@anu.edu.au.

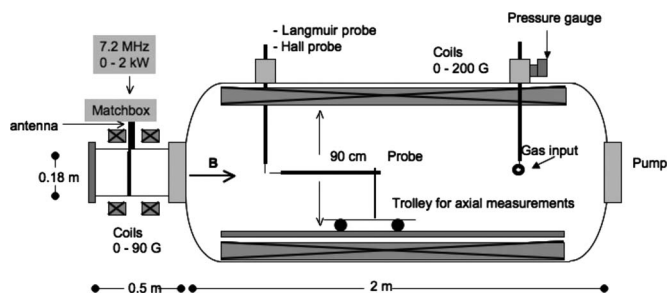


FIG. 1. A schematic of the WOMBAT plasma device.

hertz range that were associated with the various types of mode coupling in helicon discharges and were the result of plasma gas pumping. More recently chaos, turbulence, and drift waves have been investigated in the magnetically confined plasma device VINETA.^{9,21}

In this paper we report on periodic pulling and entrainment of a low-frequency instability observed in the high-density ($>10^{12}$ cm⁻³), high-beta ($\beta > 1$) plasma system WOMBAT.²²

II. EXPERIMENTAL SETUP

A. WOMBAT

The experiments were conducted in the large volume plasma system, WOMBAT (Fig. 1). It consists of a glass source tube of 50 cm long and 18 cm in diameter attached on axis to a large stainless steel diffusion chamber 200 cm long and 90 cm inner diameter, as shown in Fig. 1. A steady axial magnetic field is maintained by a set of external solenoids surrounding the source and a large solenoid inside the diffusion chamber. In these experiments, the source solenoids were not used as it was found very difficult to couple a plasma into the whole length of the diffusion chamber. As a result the magnetic field was highly uniform inside the diffusion chamber but divergent in the source having a value of only a few gauss of the central field at the end of the source. The maximum achievable magnetic field in the diffusion chamber was 200 G. Radio-frequency (rf) powers up to 2 kW at a driving frequency of 7.2 MHz were applied to one end of a single loop antenna via a matching network, while the other end was kept grounded. The antenna is 20 cm in diameter, 1 cm wide, and 0.3 cm thick, and was positioned around the outside of the glass source tube, directly below the matching box. It was located 30 cm from the source/diffusion chamber interface. Forward and reflected power measurements were made as a function of time by a directional coupler between the matching network and the rf generator. A base pressure of 4×10^{-6} Torr was maintained by a pumping system consisting of a turbomolecular pump and rotary pump attached to the diffusion chamber end opposite the source. Operating pressures of argon gas up to 3 mTorr were set using a mass flow controller and the pressure was monitored using an ionization gauge and a convectron in the diffusion chamber near the pump end. The gas input is located near the pump to minimize any potential bulk flow.

B. Diagnostics

In WOMBAT, interchangeable Langmuir probes can be inserted from the source tube end or at various axial positions in the diffusion chamber corresponding to $z=50$ cm and $z=150$ cm from the source. These probes are attached to WOMBAT via a computer controlled translation system with a spatial resolution of 1 mm. A further probe could move axially along the length of the diffusion chamber. For the present measurements ion density perturbations were detected by biasing the probe at -54 V. The ion saturation portion of the Langmuir $I(V)$ curve is far less sensitive to rf effects compared to the electron saturation part. It is found that, for the present measurements, the Langmuir probe can experience a significant amount of heating in the high-density plasma discharge, which melts rf compensating components, used for filtering rf fluctuations. Furthermore, sufficiently large rf inductors will require large probe stems which will significantly perturb the surrounding plasma. Hence an uncompensated shielded Langmuir probe was employed for this study. For the present high-density plasma discharge in the thin sheath regime (the probe sheath is much less than the probe radius), the effect that the rf fluctuations have on the floating potential, and hence the $I(V)$ characteristics was found to be negligible. It was found that the floating potential would need to vary by up to 40 V to change the positive ion density by 10%. Furthermore, the effect that the instability will have on the time-averaged $I(V)$ characteristics will be far more dominant than the rf fluctuations.

Data acquisition and fast Fourier transforms of the time varying probe signal were managed with a National Instruments high-speed digitizer having a sampling rate of 100 MHz that was controlled via a LABVIEW diagnostic system. Although the frequency spectrum was investigated for frequencies up to 10 MHz, here we are interested only in low-frequency oscillations of a few kilohertz.

External modulation of the instability was achieved by varying the amplitude of the rf drive frequency at frequencies less than 10 kHz. For this a frequency generator with a resolution of 100 Hz was employed. The rf amplitude modulation could be varied up to 100% of the rf signal. This allowed for the instability observed in the plasma discharge to be investigated for nonlinear behavior.

III. RESULTS AND DISCUSSION

A. Plasma instability characteristics

When operating above an input power of 900 W and a magnetic field of 30 G a column of 10 cm full width at half maximum of bright blue light (due to Ar II radiation) is observed along the axis of the diffusion chamber. With this blue mode, the plasma density is axially very uniform, decreasing by 10% over 1 m in the diffusion chamber at low pressures (<0.5 mTorr). However, the radial profiles of the plasma density and electron temperature are not uniform with the plasma density decreasing by 30% over 15 cm.²² Cross-field diffusion is strongly modified with increasing magnetic field, where the plasma density increases in the plasma center and decreases at the plasma edge. The decrease in the density at

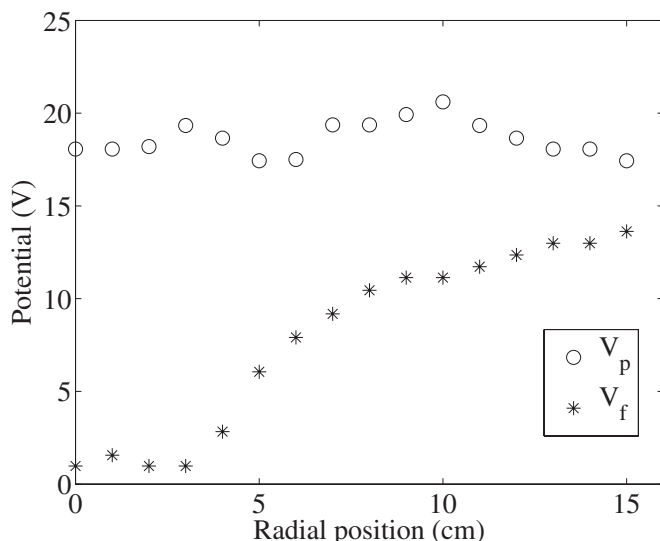


FIG. 2. The radial variation of the plasma potential (open circles) and the floating potential (asterisk) at 68 G, 0.6 mTorr, and 1708 W.

the edge is a result of a decrease in the radial plasma diffusion. With increasing magnetic field strength there is an increase in plasma confinement and axial diffusion is dominant. The radial variation of the plasma and floating potentials are shown in Fig. 2. The plasma potential is observed to be relatively flat across the diffusion chamber radius while the floating potential is a minimum at the center and increases with increased distance from the radial center. These results are similar to Perry *et al.*²³ in a much smaller helicon system. Since the electron temperature falls off rapidly with radius, the relationship between $V_p - V_f$ and the electron temperature holds. These profiles imply that the ion loss is due to thermal ions diffusing classically and suggests that the radial potential has a negative slope which would serve to confine the ions electrostatically.

Temporal phenomena in the ion saturation current were observed in the diffusion chamber of WOMBAT for magnetic fields above 30 G and for gas pressures less than 1.5 mTorr. Ion density fluctuations were observed in the plasma by biasing the Langmuir probe at -54 V and the frequency spectra were recorded. A typical trace of the instability amplitude is plotted on the same graph as the radial plasma density measured with the same Langmuir probe (Fig. 3). The unstable behavior of the plasma manifests itself in the form of enhanced levels of fluctuations at the plasma blue core center with a second peak occurring in the region of maximum density gradient indicating that the instability has resistive drift-type characteristics.⁷ A similar dependence is observed for the radial variation of the floating potential (inset of Fig. 3). The frequency of the instability was found to be in the range of 800 Hz to several kilohertz and was dependent on the plasma operating conditions of input power, gas pressure, and magnetic field. For the present operating conditions of input power of 1708 W, a magnetic field of 68 G, and a gas pressure of 0.6 mTorr, the plasma density is $\approx 10^{13}$ cm^{-3} in the center, while the electron temperature is ≈ 5 eV.²² An estimate of the axial wavelength of an ion acoustic wave yields a few meters for the conditions of the

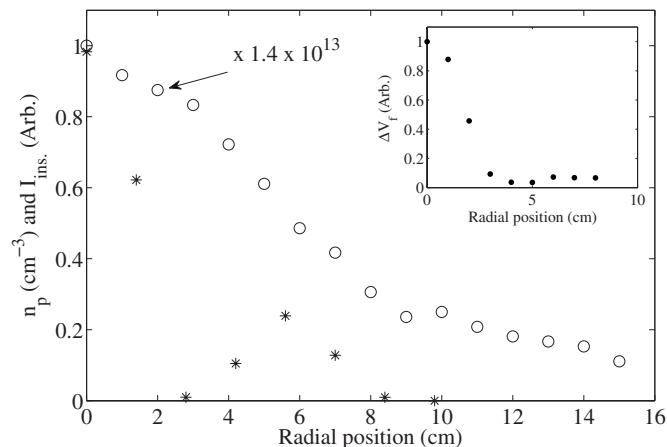


FIG. 3. The radial variation of the plasma density (open circles) and the amplitude of density fluctuations (asterisk) at 68 G, 0.6 mTorr, and 1708 W. The inset figure shows the radial variation of the amplitude of floating potential fluctuations.

experiments and that coupled with the instability maximum being in the center of the discharge strongly suggests that we are dealing with an ion acoustic instability driven azimuthally by the radial density gradients of the plasma column. The flat plasma potential profile across the radius (Fig. 2) rules out a Kelvin–Helmholtz-type instability.²⁴ It should also be noted that, under the present conditions, it is not expected that the electron temperature changes significantly in the time scale of the instability. Further measurements are currently underway to verify this phenomenon and will be presented in a future publication. Below we discuss nonlinear phenomena that occur when an external signal is applied to the plasma discharge that are indicative of a forced van der Pol system.

B. van der Pol plasma dynamics

When an external signal with a frequency f_e is applied to the plasma system with an internal instability of frequency f_0 , various nonlinear phenomena occur. For $f_e \ll f_0$, no interaction between the two oscillations takes place and both signals are observed at their respective frequencies in the frequency spectrum. However, if the external frequency is increased to $f_e < f_0$, then kept constant and the external amplitude varied, periodic pulling is observed. By further increasing the amplitude modulation, there is a frequency shift in the instability frequency toward the external frequency. This is the incomplete entrainment of the plasma instability, whereby the instability gets pulled toward the driving frequency but stops short of complete entrainment. Typical frequency spectra displaying the experimentally observed pulling phenomenon are shown in Fig. 4. The solid line corresponds to a rf amplitude modulation of 5% and the dashed line to 20%, with the driving frequency maintained at $f_e = 3.8$ kHz. The power spectra are in a quasiperiodic state and have two qualitatively different components; the driving frequency, f_e , and the free running oscillator (instability) frequency, f_0 . As the modulation is increased from 5% to 20% the instability frequency is pulled closer to the drive frequency, moving from 5 to 4.7 kHz.

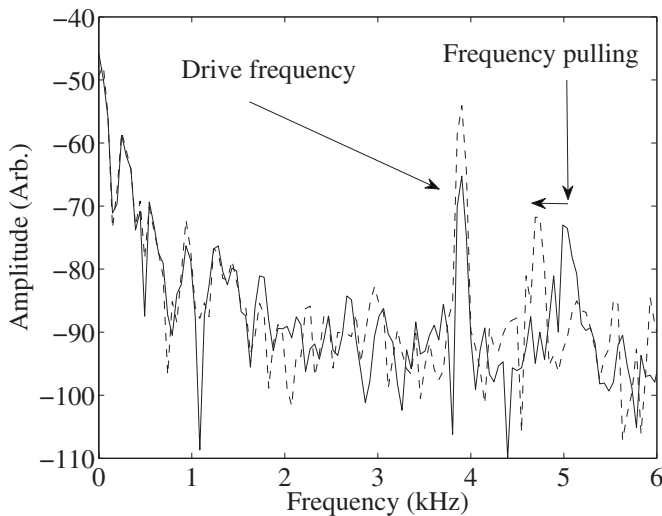


FIG. 4. The experimental frequency spectra displaying periodic pulling. The solid line corresponds to a rf amplitude modulation of 5% and the dashed line to 20%, with the driving frequency maintained at $f_e=3.8$ kHz.

The phenomena of frequency pulling and entrainment are shown in a plot of the observed spectral frequencies below 5 kHz versus applied frequency in Fig. 5. The operating conditions are an input power of 1200 W, a magnetic field of 58 G, and a gas pressure of 0.8 mTorr. As f_e approaches 2 kHz, frequency pulling commences and f_0 decreases. For the region, $1.8 \text{ kHz} < f_e < 2.5 \text{ kHz}$, there is a sharp decrease in the instability frequency from 2.9 to 2.5 kHz due to periodic pulling. It is observed that entrainment of the two signals commences at a defined frequency and, as discussed below, this critical frequency depends on the amplitude of the external signal. The critical frequency $f_e=2.5$ kHz is where the instability is captured and complete entrainment of the instability occurs. This region spans from 2.5 to 3.3 kHz. The other critical frequency of $f_e=3.4$ kHz is when the instability reappears. When the instability becomes completely en-

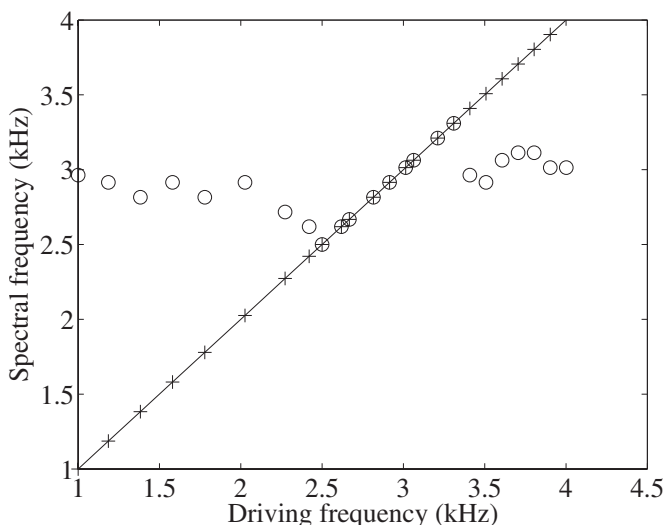


FIG. 5. The dependence of the instability frequency on the externally applied frequency. When the applied frequency, f_e (crosses) approaches the instability frequency, f_0 (open circles), f_0 is pulled toward f_e . At the critical frequency, $f_e=2.5$ kHz entrainment occurs.

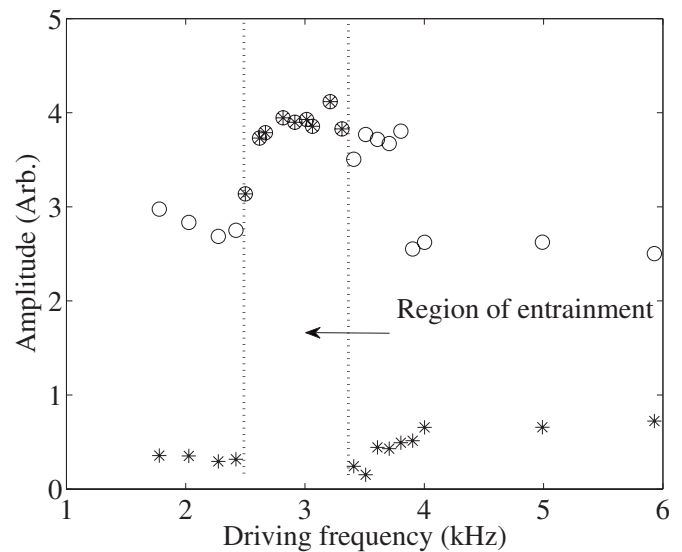


FIG. 6. The dependence of the instability amplitude (asterisk) and the external signal amplitude (open circles) on the externally applied frequency.

trained (Fig. 5), only the external frequency peak is observed in the spectrum. Here the drive signal essentially captures the instability so that the instability frequency can be controlled; the ratio between the free-running oscillator frequency and the driver frequency remains constant while the driving frequency is varied within a certain interval.

With the amplitude of the external signal kept constant and the external frequency, f_e , swept, the amplitude of both frequencies were recorded (Fig. 6). The asterisk represents the instability amplitude and the open circles represent the external amplitude. At low frequencies ($f_e < 2$ kHz) there is little or no interaction between the two signals. At the frequency where entrainment commences ($f_e=2.5$ kHz), only the drive frequency is observed in the frequency spectrum. The amplitude of this external oscillation is observed to increase dramatically over the entrainment region. The entrainment region in Fig. 6 is around 1 kHz. By further increasing f_e , both frequencies remain synchronized until the external frequency reaches a critical value, at which point the internal instability frequency reappears. It is observed that although the instability returns at $f_e \approx 3.4$ kHz, the external amplitude remains high until $f_e \approx 3.8$ kHz, showing that there is still a strong interaction occurring between the two oscillations.

A forced van der Pol system can be described by the following equation:

$$\frac{d^2x}{dt^2} - (\alpha - \beta x^2) \frac{dx}{dt} + \omega_0^2 x = A \omega_0^2 \cos(\omega_e t), \quad (2)$$

where x is the displacement of the oscillating physical quantity (plasma potential or density) from its equilibrium position, β determines the degree of nonlinear saturation, α is the linear growth rate, t is time, A is the external force amplitude, and $f_0 = \omega_0/2\pi$ is the frequency of the free-running oscillator (internal frequency), in this case the instability frequency. The frequency of the external force is given by $f_e = \omega_e/2\pi$. If $(\alpha - \beta x^2) < 0$, the oscillation is damped. When $(\alpha - \beta x^2) > 0$, the oscillation amplitude will grow exponentially with time until the term in brackets becomes negative

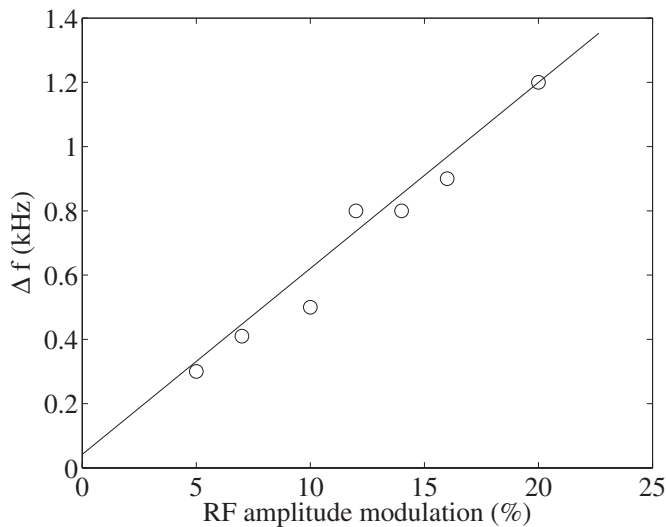


FIG. 7. The width of the entrainment region, Δf plotted against the rf amplitude modulation. The line represents Eq. (3).

again with the growth rate determined by the coefficient, α . With no damping and no external force the oscillator will oscillate with the frequency $f_0 = \omega_0/2\pi$.

For this forced van der Pol system, when $f_e \ll f_0$, there is no interaction between the two frequencies. In a similar manner to the experimental results, if the external frequency is then increased to approach the internal frequency, the two oscillations begin to interact, with the internal frequency shifting toward the externally applied frequency. This frequency pulling¹⁵ is a result of the incomplete entrainment of an oscillatory nonlinear system by a periodically varying driving force, and is observed experimentally when the instability jumps between the driven and natural frequencies of the system. Increasing the external frequency further results in the internal frequency merging with the drive frequency, a phenomenon that has previously been referred to as mode locking, phase locking, synchronization,¹³ or frequency entrainment.¹⁴ This phenomenon is displayed clearly in the experimental results presented here.

The strongest evidence that the system can be classified as a forced van der Pol oscillator is good agreement between the width dependence of the frequency entrainment region on the external amplitude modulation of the rf signal and that predicted by theory. The width of the entrainment region is proportional to the external force amplitude A (Ref. 12) and is given by

$$\Delta\omega = \omega_2 - \omega_1 = \omega_0 \frac{A}{a_0}. \quad (3)$$

The results are displayed in Fig. 7. The width of the entrainment region varies directly with the amplitude of the driving force. This linear dependence is predicted by Eq. (3) (shown by the line in Fig. 7), indicating that a van der Pol oscillatory system is present. For set values of the external amplitude modulation, there are a range of frequencies for which entrainment occurs. The range of driving amplitudes capable of entraining the system has a minimum which varies with frequency and has no observed maximum.

Periodic doubling bifurcations can also occur in frequency entrained states when the driving frequency has a strong amplitude. Here, the periodicity of the time evolution is doubled and in the power spectrum subharmonic components appear. These components are weak as they are dominated by the initial periodic state.^{4,14}

IV. CONCLUSIONS

The investigation presented in this paper deals with the periodic pulling and frequency entrainment of a low-frequency instability observed in a high-density, high-beta argon plasma. The forced van der Pol oscillator model was shown to give a good description of the nonlinear dynamics. When an external signal is applied to the rf input power with a frequency close to the instability frequency, nonlinear phenomena of the instability occur. It was shown that the frequency window for entrainment increases linearly with increasing amplitude of the external force, indicative of a forced van der Pol oscillatory system. Once entrainment commences, the spectrum consists of only a single peak at the external driving frequency.

These results provide important insight into the dynamics and control of instabilities occurring in magnetically confined high-density, high-beta plasma that may have application in fusion plasma. Furthermore, the present work may provide some insight into astrophysical plasma phenomena whereby solar wind turbulence may be due to an ensemble of Alfvén and ion acoustic waves that are entrained within the solar wind flow.

¹B. van der Pol, *Radio Review* **1**, 701 (1920).

²B. van der Pol, *Philos. Mag.* **43**, 700 (1922).

³B. van der Pol and J. van der Mark, *London, Edinburgh Dublin Philos. Mag. J. Sci.* **6**, 763 (1928).

⁴R. W. Boswell, *Plasma Phys. Controlled Fusion* **27**, 405 (1985).

⁵R. W. Boswell and M. Giles, *J. Plasma Phys.* **33**, 59 (1985).

⁶C. S. Corr, N. Plihon, P. Chabert, O. Sutherland, and R. W. Boswell, *Phys. Plasmas* **11**, 4596 (2004).

⁷H. W. Hendel, T. K. Chu, and P. A. Politzer, *Phys. Fluids* **11**, 2426 (1968).

⁸W. Horton, *Rev. Mod. Phys.* **71**, 735 (1999).

⁹C. Schroder, O. Grulke, T. Klinger, and V. Naulin, *Phys. Plasmas* **12**, 042103 (2005).

¹⁰J. Perez, W. Horton, K. Gentle, W. Rowan, K. Lee, and R. Dahlburg, *Phys. Plasmas* **13**, 032101 (2006).

¹¹R. W. Boswell and P. J. Christiansen, *Phys. Fluids* **16**, 692 (1973).

¹²B. E. Keen and W. H. W. Fletcher, *Phys. Rev. Lett.* **23**, 760 (1969).

¹³B. Keen and W. Fletcher, *J. Phys. D: Appl. Phys.* **3**, 1868 (1970).

¹⁴T. Klinger, F. Greiner, A. Rohde, A. Piel, and M. Koepke, *Phys. Rev. E* **52**, 4316 (1995).

¹⁵R. H. Abrams, E. Yadlowsky, and H. Lashinsky, *Phys. Rev. Lett.* **22**, 275 (1969).

¹⁶D. Block, A. Piel, C. Schroder, and T. Klinger, *Phys. Rev. E* **63**, 056401 (2001).

¹⁷R. W. Boswell, *Plasma Phys. Controlled Fusion* **26**, 1147 (1984).

¹⁸M. Light, F. Chen, and P. Colestock, *Phys. Plasmas* **8**, 4675 (2001).

¹⁹M. Light, F. Chen, and P. Colestock, *Plasma Sources Sci. Technol.* **11**, 273 (2002).

²⁰A. Degeling, T. Sheridan, and R. W. Boswell, *Phys. Plasmas* **6**, 1641 (1999).

²¹C. Franck, O. Grulke, and T. Klinger, *Phys. Plasmas* **9**, 3254 (2002).

²²C. S. Corr and R. W. Boswell, *Phys. Plasmas* **14**, 122503 (2007).

²³A. Perry, G. Conway, R. Boswell, and H. Persing, *Phys. Plasmas* **9**, 3171 (2002).

²⁴D. L. Jassby, *Phys. Fluids* **15**, 1590 (1972).